EUROPEAN ORGANIZATION FOR NUCLEAR RESEARCH

CERN-EP/83-28
17 February 1983

THE REACTION $\gamma p \rightarrow p\omega\pi^+\pi^-$ FOR PHOTON ENERGIES OF 25-50 GeV

Bonn[1]-CERN[2]-Glasgow[3]-Lancaster[4]-Manchester[5]-Paris VI[6]-Rutherford[7]-Sheffield[8] Collaboration

M. Atkinson[7], T.J. Axon[5], D. Barberis[5], T.J. Brodbeck[4], G.R. Brookes[8], J.J. Bunn[8], P.J. Bussey[3], A.B. Clegg[4], J.B. Dainton[3], M. Davenport[7], B. Dickinson[5], B. Diekmann[1], A. Donnachie[5], R.J. Ellison[5], P. Flower[7], P.J. Flynn[4], W. Galbraith[8], K. Heinloth[1], R.C.W. Henderson[4], R.E. Hughes-Jones[5], J.S. Hutton[7], M. Ibbotson[5], H.P. Jakob[1], M. Jung[1], M.A.R. Kemp[7], B.R. Kumar[7], J. Laberrigue[6], G.D. Lafferty[5], J.B. Lane[5], J.C. Lassalle[2], J.M. Lévy[6], V. Liebenau[1], R.H. McClatchey[8], D. Mercer[5], J.A.G. Morris[7], J.V. Morris[7], D. Newton[4], C. Paterson[3], G.N. Patrick[2], E. Paul[1], C. Raine[3], M. Reidenbach[1], H. Rotscheidt[1], A. Schlösser[1], P.H. Sharp[7], I.O. Skillicorn[3], K.M. Smith[3], K.M. Storr[2], R.J. Thompson[5], Ch. de la Vaissière[6], A.P. Waite[5] and T.P. Yiou[6]

(The Omega Photon Collaboration)

ABSTRACT

Measurements of the reaction $\gamma p \rightarrow p\omega\pi^+\pi^-$ are reported for photon energies 25-50 GeV. Particular attention is paid to $\omega\pi^+\pi^-$ masses < 2 GeV. A search is made for ω' or ϕ' partners of the $\rho'(1600)$. Evidence is presented against the existence of narrow states and against the production of a broad state by an s-channel helicity conserving mechanism.

(Submitted to Nuclear Physics B)

1. INTRODUCTION

Searches for vector mesons, V, have been made in diffractive dissociation in photoproduction

$$\gamma p \to pV \tag{1}$$

and in electron-positron annihilation

$$e^+e^- \to V \tag{2}$$

with the results of the two processes being related by the Vector Dominance Model (VDM). Detailed studies have been made of production of the ρ, ω, and ϕ in both processes (a summary of measurements of electron-positron annihilation and comparison with photoproduction at lower photon energies is made by Bauer et al. [1]; photoproduction measurements at higher energies have since been reported [2]).

Information on higher mass vector meson nonets is more fragmentary. A $\rho'(1600)$ has been observed, decaying primarily into $\pi^+\pi^-\pi^+\pi^-$ and $\pi^+\pi^-\pi^0\pi^0$ states [3-8]. From measurements of these decay modes widths of the $\rho'(1600)$ in the range 0.4-0.6 GeV are indicated, with uncertainty due to the problem of separating other contributions to production of the 4π states (indeed the possibility of such contributions has been ignored in some analyses [6-8]). The uncertainty in width is complicated by observation [9,10] of a peak in diffractively photoproduced $\pi^+\pi^-$ with the same mass but with a width of $\sim$ 0.25 GeV. This latter result is supported by the indication of a $J^\pi =$ $= 1-$ state of width $\sim$ 0.2 GeV in those analyses of $\pi\pi$ scattering which are favoured by a recent polarized target experiment [11,12]. A candidate for the ϕ' member of the same nonet has been reported in $\omega\pi^+\pi^-$, $K\bar{K}$ and $K^0_sK^\pm\pi^\mp$ states produced in electron-positron annihilation [13-15]. In particular a Breit-Wigner formula has been fitted [13] to the $\omega\pi^+\pi^-$ mass spectrum with a peak at 1.657 ± 0.013 GeV and a width of 0.136 ± 0.046 GeV. It is usually assumed that a ϕ' state would mainly decay into states involving K mesons and that, as a major decay of the $\rho'(1600)$ is into $\rho\pi\pi$, a similar major decay of the ω' member of the same nonet would be into $\omega\pi\pi$. Hence a global fit has been made [16] to the $\omega\pi^+\pi^-$, $K\bar{K}$ and $K^0_sK^\pm\pi^\mp$ mass spectra from electron-positron annihilation, assuming contributions from the $\rho'(1600)$ and the corresponding ϕ' (taken to have a width $\sim$ 0.15 GeV) and ω' (taken to have a width ∿ 0.5 GeV). The resulting interference between ϕ' and ω' generated a single peak of width ∿ 0.35 GeV in $\omega^0\pi^+\pi^-$.

Earlier work [17] from the CERN WA4 experiment, on the reaction

$$\gamma p \rightarrow p\omega\pi^+\pi^- , \qquad (3)$$

reported a broad peak in the $\omega\pi^+\pi^-$ mass spectrum at a mass ∿ 1.7 GeV with a width ∿ 0.5 GeV, produced with a cross-section which was consistent with expectation for the ω' partner of the $\rho'(1600)$, together with production of jet-like $\omega\pi^+\pi^-$ systems of masses $\gtrsim$ 2 GeV.

The present work, from the CERN WA57 experiment, is a further study of reaction (3) with a factor of three increase in data. The results agree with the conclusions of the previous experiment, and extend them to show that the $\omega\pi^+\pi^-$ systems in the broad peak at 1.7 GeV are largely in a $J^\pi =$ = 1- state, but are produced with an alignment differing from s-channel helicity conservation (SCHC), so arguing against this broad peak being due to the ω' partner of the $\rho'(1600)$. The results are inconsistent with the narrow peak indicated by electron-positron annihilation [13].

2. EXPERIMENTAL PROCEDURE

This experiment used an 80 GeV electron beam to produce tagged photons of energies 20-70 GeV [18]. The particles resulting from interaction of these photons in a 60 cm liquid hydrogen target were detected in the Omega spectrometer, equipped with multiwire proportional chambers, drift chambers, a threshold gas Cerenkov counter and a large aperture photon detector. The trigger required between two and five charged particles to be detected in a forward MWPC together with at least one gamma-ray, with energy $\gtrsim$ 2 GeV, to be detected in the photon detector. Off-line software required two gamma-rays to be reconstructed to form a π^0 meson and there to be four or five charged particles consistent with $\pi^+\pi^-\pi^+\pi^-$ or $\pi^+\pi^-\pi^+\pi^- p$, respectively. Events from the reaction

$$\gamma p \rightarrow \pi^+\pi^-\pi^+\pi^-\pi^0 p \qquad (4)$$

were selected by a cut on

$$\Delta E = \text{incident photon energy} - \Sigma(\pi \text{ meson energies}) .$$

The ΔE distribution for reaction (3) is shown in Fig. 1, where $\omega\pi^+\pi^-$ states have been selected by the procedure described in the next section. As well as the evident peak due to reaction (3), there is a background due to other processes where further, unobserved, particles have been produced. This background was investigated previously [17], and it was shown that a cut requiring -1.5 GeV $< \Delta E < 1.0$ GeV makes a good selection of reaction (3). The background due to other processes is estimated to be $\sim$ 25%.

A Monte Carlo simulation programme has been used to study the acceptance of the apparatus. This programme simulates the effects of the detectors and of the analysis programmes on both charged particles and gamma-rays; in particular a full simulation of showering in the photon detector and the resulting effects on the analysis programme was made. Two models for the $\omega\pi^+\pi^-$ systems ($\omega\pi\pi$ phase space and $B^{\pm}\pi^{\mp}$) were studied in detail and a third ($\omega\varepsilon$, where ε, as described previously [4], denotes the low energy s-wave $\pi\pi$ interaction determined by the measured phase shifts) in outline. No significant difference was found between the acceptances calculated for these models, so results for $\omega\pi\pi$ phase space are shown. The dependence of the results on most experimental variables was not changed in any significant way by acceptance, so these distributions are presented without correction. The acceptance does have a major effect on the shape of the ω meson production angular distributions in Fig. 5, and there corrections for acceptance are made.

3. RESULTS

Figure 2 shows the measured $\pi^+\pi^-\pi^0$ mass spectrum (four entries/event). A fit to the mass range 0.45-0.95 GeV using two Breit-Wigner formulas and a cubic polynomial background gives:

for the η meson: peak at 0.5490 GeV, width = 0.017 ± 0.001 GeV

for the ω meson: peak at 0.7847 GeV, width = 0.029 ± 0.001 GeV .

These peak positions are in good agreement with the world average values [19], and the widths agree with the resolutions found by simulation. Events corresponding to ω mesons were taken to be those with a $\pi^+\pi^-\pi^0$ mass in the range 0.75-0.82 GeV, and a background deduced from sidebands (masses

0.715-0.75 or 0.82-0.855 GeV) was subtracted. For those relatively rare cases where an event had two or more 3π masses in this region each identification was treated as an independent event; this is statistically correct except for the neglect of the error correlation, which is a small effect. This background subtraction procedure was tested by studying the parameter

$$\lambda = \frac{|\underset{\sim}{p}^{+} \times \underset{\sim}{p}^{-}|^{2}}{\frac{3}{4}\left[\frac{1}{9} M^{2} - \frac{1}{3}\left(2m_{c}^{2} + m_{0}^{2}\right)\right]^{2}}$$

(where $\underset{\sim}{p}^{+}$, $\underset{\sim}{p}^{-}$ denote the three momenta of the π^{+} and π^{-} in the 3π CM system, M denotes the mass of the 3π, m_c and m_0 the masses of charged and neutral π mesons), which measures the radial distribution of ω-meson decays over the Dalitz plot. Figure 3 shows the measured λ distributions; the distribution from the sidebands is flat, corresponding to uniform population of phase space, while the distribution for ω mesons, after subtraction of background, rises linearly from zero as is expected [20].

Figure 4 shows the measured $\omega\pi^{+}\pi^{-}$ mass spectrum, together with the calculated variation of acceptance with mass. (The dashed and dotted curves on Fig. 4 are discussed later.) This mass spectrum shows no indication of any narrow peak.

The t-distributions are found to be exponential. On fitting with A exp (bt), for $0 < |t| < 1$ (GeV/c)^2, one finds:

$$1.0 \text{ GeV} < M(\omega\pi\pi) < 2.0 \text{ GeV}: \quad b = 7.04 \pm 0.63$$

$$2.0 \text{ GeV} < M(\omega\pi\pi) < 3.5 \text{ GeV}: \quad b = 4.62 \pm 0.28 \ .$$

The distributions indicate a peripheral production mechanism, consistent with expectation for diffractive dissociation. The decrease of b with increasing mass is typical of other diffractive dissociation processes.

Figure 5 shows the measured distributions of angle of production of the ω meson, with respect to the s-channel helicity axis in the $\omega\pi^{+}\pi^{-}$ CM system, for two ranges of $\omega\pi\pi$ mass: (a) 1.0-2.0 GeV; (b) 2.0-3.5 GeV. These angular distributions have been corrected for acceptance: the correction used is shown. The results in Figs. 4 and 5 demonstrate the same conclusions as were reached in the previous experiment [17]. For $M(\omega\pi\pi) < 2.0$ GeV ω meson production is isotropic, while for $M(\omega\pi\pi) < 2.0$ GeV there is peaking consistent with production of jet-like $\omega\pi\pi$ systems.

The $\omega\pi^{\pm}$ mass spectrum shows a peak of mass and width consistent with being due to the B meson. Investigation shows that production of $B^{\pm}\pi^{\mp}$ states is largely confined to the range $1.6 < M(\omega\pi\pi) < 2.0$ GeV. The angular distribution of the B meson, with respect to the s-channel helicity axis in the $\omega\pi^{+}\pi^{-}$ CM system, shows a strong backward peaking; effectively all the B mesons are at $\cos\theta_B < -0.5$, where θ_B denotes the angle between the s-channel axis and the direction of the B meson. These results are demonstrated in Fig. 6, which shows $\omega\pi^{\pm}$ mass spectra for three ranges of $\omega\pi\pi$ mass, and in Fig. 7, which shows $\omega\pi^{\pm}$ mass spectra for two ranges of $\cos\theta_B$ for 1.6 GeV $< M(\omega\pi\pi) <$ 2.0 GeV. The peaking in the $B\pi$ mass distribution and the asymmetric angular distribution are interpreted as indicating production of $B\pi$ by some direct mechanism which is producing a threshold peak. It is noted that the peaking in the angular distribution is in the opposite direction to that expected for one obvious possibility, namely a Deck mechanism involving π meson exchange (see, for example, the review by Berger [21]).

The spin and parity of the $\omega\pi^{+}\pi^{-}$ system are now discussed. As an $\omega\pi\pi$ system from dissociation of a photon has $C = -1$, the $\pi\pi$ system has $C = +1$ and therefore even ℓ. This would be expected to be largely $\ell = 0$, due to the strong final state interaction in that state at low $\pi\pi$ masses, and this is supported by the rapid rise observed at threshold in the $\pi\pi$ mass spectrum, which, for 1.0 GeV $< M(\omega\pi\pi) <$ 2.0 GeV, is shown in Fig. 8. For $\ell = 0$ there is then a correlation between L, the angular momentum of the ω meson and the $\pi\pi$ pair, and the J^{π} of the $\omega\pi\pi$ system. For example:

L	J^{π}
0	1-
1	0+,1+,2+.

L can be determined from the distribution of events on the $\omega\pi\pi$ Dalitz plot, due to the factor q^{2L} (where q is the three momentum of the ω meson in the

$\omega\pi\pi$ CM system) and from the distribution of the angle, θ_H, of the normal to the ω meson decay plane with respect to the direction of the $\pi\pi$ system in the ω meson CM system, which should be (for example)

$J^\pi = 1-$: isotropic

$J^\pi = 0+$: $\cos^2 \theta_H$

$J^\pi = 1+$: $\sin^2 \theta_H$.

Therefore distributions have been studied of $\cos \theta_H$ and of $T_\omega/T_{\omega\max}$, where T_ω denotes the kinetic energy of the ω meson in the $\omega\pi\pi$ CM system and $T_{\omega\max}$ denotes the maximum value of T_ω allowed for that $\omega\pi\pi$ mass. The measured distributions of $T_\omega/T_{\omega\max}$ are shown in Fig. 9: Fig. 9a for $1.3 < M(\omega\pi\pi) <$ < 1.6 GeV and Fig. 9b for $1.6 < M(\omega\pi\pi) < 2.0$ GeV. Comparison is made with calculations for $\omega\pi\pi$ phase space for Fig. 9a and for a combination of $\omega\pi\pi$ phase space and $B\pi$ (in the ratio determined from Fig. 6b) in Fig. 9b, for both $L = 0$ and 1 in each case. These results show better agreement with $L = 0$. The measured distributions of $\cos \theta_H$ were fitted with $a(1+ b \sin^2 \theta_H)$, giving

$1.3 < M(\omega\pi\pi) < 1.6$ GeV: $b = -0.33 \pm 0.25$

$1.6 < M(\omega\pi\pi) < 2.0$ GeV: $b = 0.20 \pm 0.39$.

In both mass ranges these measurements of $T_\omega/T_{\omega\max}$ and of $\cos \theta_H$ are consistent with $J^\pi = 1-$, and in the higher mass range exclude other major contributions. Finally it is noted that the isotropy of the angular distribution in Fig. 5a is consistent with $L = 0$.

Hence the spin alignment of the $\omega\pi\pi$ state is studied under the assumption that only $J^\pi = 1-$ contributes. Then the alignment of the $\omega\pi\pi$ state is transferred to the ω meson, which can then be deduced from the distribution of the angle, θ_N, between the direction of the normal to the ω meson decay plane and the s-channel axis in the ω meson CM system. Such angular distributions, for various selections, were fitted with

$$a\left[\rho_{00} \cos^2 \theta_N + \frac{1}{2}\left(1 - \rho_{00}\right) \sin^2 \theta_N\right]$$

(where ρ_{00} is a spin density matrix element) giving:

1.3 GeV < $M(\omega\pi\pi)$ < 1.6 GeV : $\rho_{00} = 0.38 \pm 0.09$

1.6 GeV < $M(\omega\pi\pi)$ < 2.0 GeV
and $\cos\theta_B > -0.5$: $\rho_{00} = 0.34 \pm 0.06$

1.6 GeV < $M(\omega\pi\pi)$ < 2.0 GeV
and $\cos\theta_B < -0.5$
and 1.25 GeV < $M(\omega\pi)$ < 1.275 GeV : $\rho_{00} = 0.33 \pm 0.16$.

The first two of these selections essentially exclude $B\pi$ production, while the third selects almost entirely $B\pi$ production. Particularly for the selections of $\omega\pi\pi$ production which is not through $B\pi$ there is significant departure from $\rho_{00} = 0$ which corresponds to SCHC alignment. As photoproduction of ρ, ω and ϕ [1,2] and of the $\rho'(1600)$ [3,4] are found to be primarily by an SCHC mechanism, it would seem that such a mechanism is typical of direct diffractive dissociation of the photon to vector mesons. Thus the observed departure from SCHC alignment argues against a major contribution to this $\omega\pi\pi$ production from the ω' partner of the $\rho'(1600)$.

Cross-sections for reaction (3) have been determined, taking into account corrections for:

i) Acceptance of apparatus and analysis programmes, as estimated by simulation.

ii) Losses of incident photons due to double bremsstrahlung in the radiator and failure in reconstructing tracks in the tagging system.

iii) ω meson decay branching ratios.

The normalization was determined by counting the number of incident photons detected by the tagging system. The cross-section for producing $\omega\pi^+\pi^-$ with a mass in the range 1.0-2.0 GeV is 82 ± 20 nb, averaged over photon energies from 25 to 50 GeV.

The energy dependence of the cross-section has been studied for photon energies in the range 25-50 GeV (the number of events above 50 GeV is small, due both to a fall in acceptance and to the rapid decrease in number of photons). The energy spectrum of the incident beam was measured by a subsidiary trigger detecting electron-positron pairs. The cross-section is found to vary as E_γ^{-n} with n = 0.7 ± 0.3, which is consistent with other similar reactions [4].

A comparison is now made with the electron-positron annihilation results [13]. States produced by electron-positron annihilation should have $J^\pi = 1-$. From fragmentation of the real photon there should be major contributions with $J^\pi = 1-$ to the states produced, but additional contributions of other J^π are possible. Hence effects seen in electron-positron annihilation could be hidden in photoproduction. However, the expected photoproduction cross-section corresponding to an observed electron-positron annihilation cross-section can be estimated by using VDM. As this procedure has been calibrated [4] by comparing measurements of production of the $\rho'(1600)$, it would be expected that such estimates would be reliable for photoproduction of the ω' and ϕ' members of the same nonet. This procedure indicated [4] a total $\rho'(1600)$ proton cross-section of 16.7 mb. Therefore, for the present comparison, we take the same cross-section for the ω' member of the nonet and a smaller cross-section, 9 mb, for the ϕ' member. As a representation of the electron-positron annihilation data [13] we take the peak, of width 0.136 GeV, fitted to the results. The dotted curve in Fig. 4 shows the expected result deduced for this peak. This calculation assumes the peak is due to a ϕ'; if an ω' were assumed the peak predicted in Fig. 4 would be higher by a factor of 3. Even if there were contributions to photoproduction additional to those due to electron-positron annihilation, the results in Fig. 4 are inconsistent with a contribution of a peak of the width and magnitude shown. The later model [16], fitted to several electron-positron reactions, assumes interference between ω' and ϕ'. In deducing the resulting photoproduction cross-section (assuming parameters which were found to fit the curve on Fig. 1a of Ref. 16) the contribution of ω' relative to ϕ' increases, to give the dashed curve shown in Fig. 4. For this calculation to be consistent with the present experiment, it is necessary to postulate an additional contribution in photoproduction turning on sharply at a mass of 1.8 GeV.

The peaking in the angular distribution of ω mesons for $M(\omega\pi\pi) >$ > 2.0 GeV, which is shown in Fig. 5b, is an indication of production of a jet-like structure, such as has also been reported in production of

$\pi^+\pi^-\pi^+\pi^-$ [4] and of $\pi^+\pi^-\pi^+\pi^-\pi^+\pi^-$ [22] states with masses greater than 2 GeV. This jet-like structure is explored further in Fig. 10, which shows the average values of p_T, written as $\langle p_T \rangle$ (where p_T is the component of momentum transverse to the t-channel axis in the $\omega\pi^+\pi^-$ CM system), as a function of $\omega\pi^+\pi^-$ mass separately for ω mesons and for π mesons. These measured values of $\langle p_T \rangle$ rise very slowly with increasing mass in contrast to the rapid rise calculated for $\omega\pi\pi$ phase space (which is shown in Fig. 10) and in accord with expectation for a jet-like structure (see comparison with a similar analysis of jet-like $\rho\pi\pi$ states [4]). A possible cause of such a jet-like structure is that a photon-Pomeron collision, at these high energies, is similar to a hadron-hadron collision and so is p_T limited (see, for example, DeGrand and Randa [23]). In this case the ω meson angular distribution would be expected to be similar to that for inclusive ρ meson photoproduction [24]. Then the major contribution to the forward peak in Fig. 5b could be due to the expected leading vector meson, but this does not provide an explanation for the smaller backward peak which is indicated both in this and previous experiments [17].

4. CONCLUSIONS

The measurements of reaction (3) reported in this paper are in good agreement with previous results [17] showing a broad mass distribution, with the ω meson produced isotropically (in the $\omega\pi^+\pi^-$ CM system), for $\omega\pi\pi$ masses < 2.0 GeV. At higher $\omega\pi\pi$ masses the ω meson is produced with an angular distribution which is forward and backward peaked.

We have assumed that a major contribution to production of $\omega\pi^+\pi^-$ is by diffractive dissociation of the photon. This assumption is supported by

i) The $J^\pi = 1-$ assignment.

ii) The relatively slow fall of the cross-section for reaction (3) with increasing photon energies.

iii) The exponential t distribution.

The study has mainly concentrated on $\omega\pi\pi$ masses < 2 GeV, with the particular interest of seeking candidates for ω' and ϕ' members of the same nonet as the ρ′(1600). It is shown that there is a major contribution with J^{π} = 1-, so it is possible to consider there may be a broad ω′ meson. However, the spin alignment of the ω meson is found to be inconsistent with production of the ωππ state by an SCHC mechanism, which is an argument against there being a major contribution from the ω′ partner of the ρ′(1600) decaying into $\omega\pi^+\pi^-$. We note that a candidate for an ω′ is reported [25] by the WA57 experiment in the $\pi^+\pi^-\pi^0$ state at a mass of 1.67 GeV.

The normalized $\omega\pi^+\pi^-$ mass spectrum is shown to be inconsistent with the narrow peak fitted to the electron-positron annihilation results.

There is a small production of Bπ states in the ωππ mass range 1.6-2.0 GeV. The Bπ angular distribution is peaked, indicating a non-resonant production mechanism. This peak is in the direction opposite to that for a pion-exchange Deck effect.

At ωππ masses > 2 GeV a jet-like structure is produced, which is similar to photoproduced ρππ states at these masses [4].

Acknowledgements

We are grateful to the Omega group at CERN for their help in running the spectrometer and providing on-line and off-line software. The work of the technical support staff in our home institutions, and the support at the computer centres at the Rutherford Appleton Laboratory, CERN, and the RHRZ at Bonn have been invaluable. We thank the SERC (UK), the BMFT (Fed. Rep. Germany), and the IN2P3 (France) for financial support.

REFERENCES

[1] T.H. Bauer, R.D. Spital, D.R. Yennie and F.M. Pipkin, Rev. Mod. Phys. 50 (1978) 261.

[2] R.M. Egloff et al., Phys. Rev. Lett. 43 (1979) 657, 1545.
D. Aston et al., Nucl. Phys. B172 (1980) 1.
D. Aston et al., Nucl. Phys. B209 (1982) 56.

[3] H.H. Bingham et al., Phys. Lett. 41B (1972) 635.

[4] D. Aston et al., Nucl. Phys. B189 (1981) 15.

[5] M. Atkinson et al., Phys. Lett. 108B (1982) 55.

[6] B. Esposito et al., Lett. Nuovo Cim. 28 (1980) 195.

[7] C. Bacci et al., Phys. Lett. 95B (1980) 139.

[8] A. Cordier et al., Phys. Lett. 109B (1982) 129.

[9] M.S. Atiya et al., Phys. Rev. Lett. 43 (1979) 1691.

[10] D. Aston et al., Phys. Lett. 92B (1980) 215.

[11] A.D. Martin and M.R. Pennington, Ann. Phys. (N.Y.) 114 (1978) 1.

[12] H. Becker et al., Nucl. Phys. B151 (1979) 46.

[13] A. Cordier et al., Phys. Lett. 106B (1981) 155.

[14] B. Delcourt et al., Phys. Lett. 99B (1981) 257.
F. Mane et al., Phys. Lett. 99B (1981) 261.

[15] F. Mane et al., Phys. Lett. 112B (1982) 178.

[16] J. Buon et al., Phys. Lett. 118B (1982) 221.

[17] D. Aston et al., Nucl. Phys. B174 (1980) 269.

[18] D. Aston et al., Nucl. Instrum. Methods 197 (1982) 287.

[19] Particle Data Group, Phys. Lett. 111B (1982) 1.

[20] S.M. Flatte et al., Phys. Rev. 145 (1966) 1050.

[21] E.L. Berger, Daresbury Report DL/R34 on Daresbury Study Weekend No. 8 (eds. J.B. Dainton and A.J.G. Rey) p. 35.

[22] D. Aston et al., Nucl. Phys. B166 (1980) 1.

[23] T.A. DeGrand and J. Randa, Phys. Lett. 110B (1982) 484.

[24] E. Kogan et al., Nucl. Phys. B122 (1977) 383.

[25] M. Atkinson et al., Photoproduction of an isoscalar 3π resonance at 1.67 GeV, submitted to Phys. Lett.

Figure captions

Fig. 1 : Measured distribution of ΔE = incident photon energy - Σ(π meson energies) for cases where $\omega^0\pi^+\pi^-$ state is observed.

Fig. 2 : Measured $\pi^+\pi^-\pi^0$ mass spectrum (four entries/event) from reaction (3).

Fig. 3 : Measured distribution of λ (as defined in text):

○ for events in ω meson peak region

× background from events in sideband regions.

Fig. 4 : Observed $\omega\pi^+\pi^-$ mass spectrum from reaction (3). The full curve shows the acceptance. The dotted and dashed curves are described in the text.

Fig. 5 : ω meson production angular distributions, with respect to the s-channel axis in the $\omega\pi^+\pi^-$ CM system, for:

a) $1.0 < M(\omega\pi\pi) < 2.0$ GeV.

b) $2.0 < M(\omega\pi\pi) < 3.5$ GeV.

These results have been corrected for acceptance; the corrections used are shown.

Fig. 6 : Measured $\omega\pi^\pm$ mass distributions (two entries/event) for:

a) $1.3 < M(\omega\pi\pi) < 1.6$ GeV.

b) $1.6 < M(\omega\pi\pi) < 2.0$ GeV.

c) $2.0 < M(\omega\pi\pi) < 2.3$ GeV.

The full curves show the distribution for $\omega\pi\pi$ phase space, normalized to the same total number of events in each case. The dashed curve, on (b), shows the results of a fit with phase space and a $B^\pm\pi^\mp$ distribution.

Fig. 7 : Measured $\omega\pi^\pm$ mass distribution for $1.6 < M(\omega\pi\pi) < 2.0$ GeV and

a) $\cos\theta_B < -0.5$;

b) $\cos\theta_B > -0.5$;

where θ_B is the angle between the s-channel helicity axis and the $\omega\pi$ direction in the $\omega\pi\pi$ CM system. The full curves show the distribution for $\omega\pi\pi$ phase space, normalized to the same total number of events in each case.

Fig. 8 : Measured $\pi^+\pi^-$ mass distribution from reaction (3) for $1.0 < M(\omega\pi\pi) < 2.0$ GeV.

Fig. 9 : Measured distributions of $T_\omega/T_{\omega\max}$, where T_ω is the ω meson kinetic energy in the $\omega\pi\pi$ CM system and $T_{\omega\max}$ is the maximum value of T_ω for that $\omega\pi\pi$ mass, for

a) $1.3 < M(\omega\pi\pi) < 1.6$ GeV.

b) $1.6 < M(\omega\pi\pi) < 2.0$ GeV.

The calculated curves are phase space distributions for

———— $L = 0$

– – – – $L = 1$

where L is the angular momentum of relative motion of ω meson and $\pi\pi$ pair. In each case the calculated curve is normalized to the same total number of events as the experiment.

Fig. 10 : Measured values of $\langle p_T \rangle$, the average value of momentum transverse to the t-channel axis in the $\omega\pi\pi$ CM system. The curves are calculated for $\omega\pi\pi$ phase space. The full lines show results and calculation for ω mesons, and the dashed lines for π mesons.

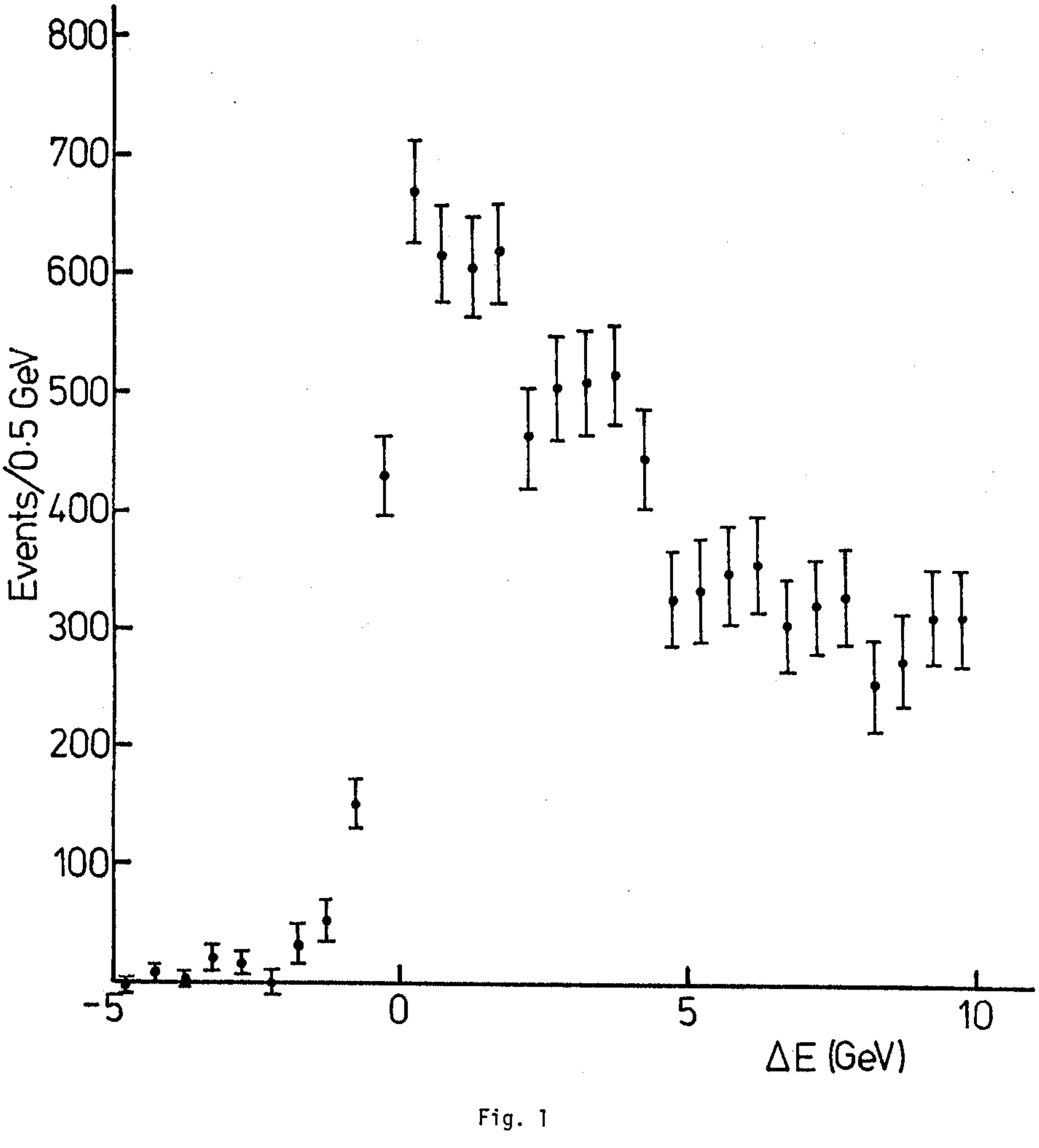

Fig. 1

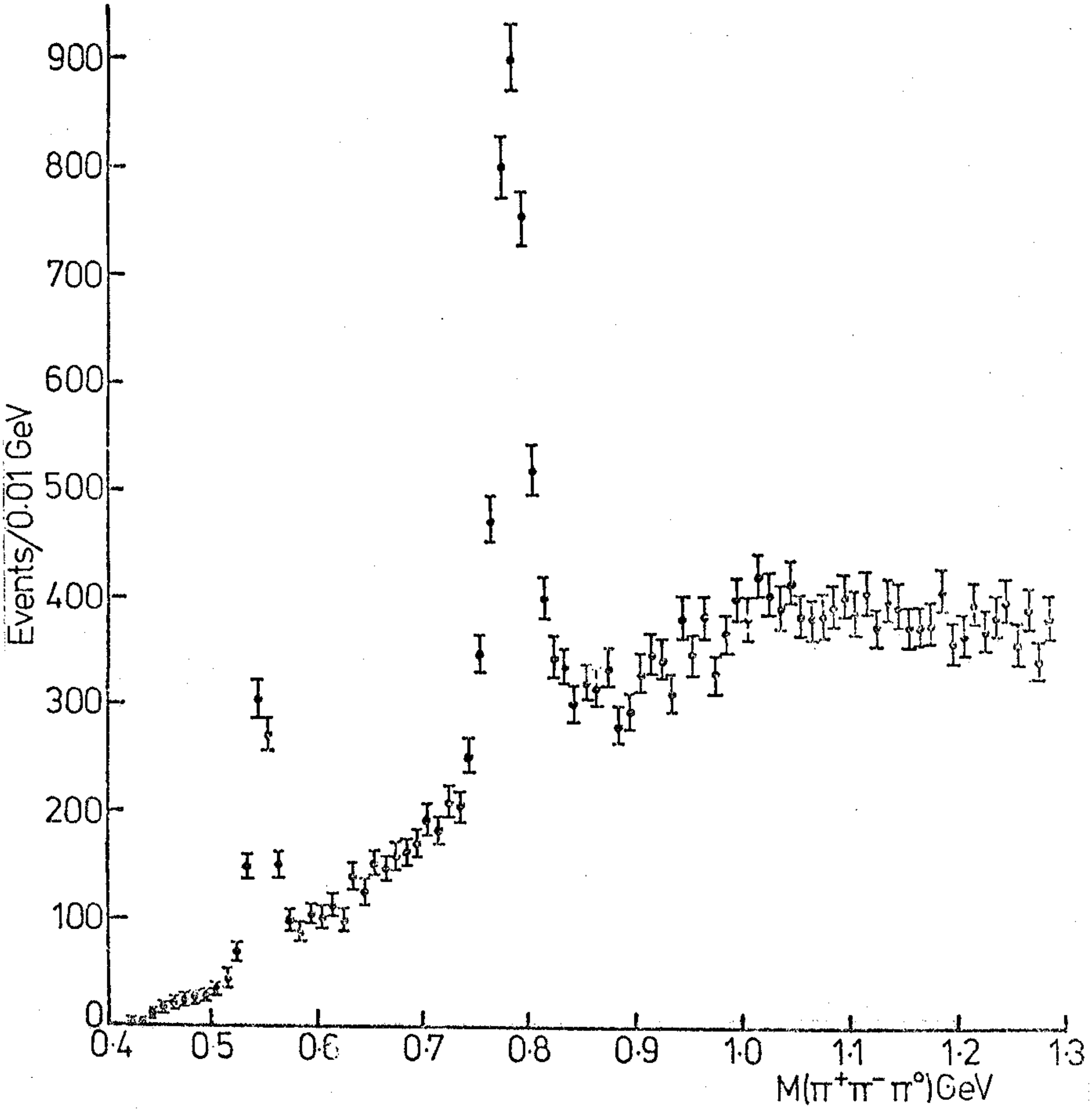
Events/0.01 GeV
900
800
700
600
500
400
300
200
100
0
0·4
0·5
0·6
0·7
0·8
0·9
1·0
1·1
1·2
1·3
M(π⁺π⁻π°)GeV

Fig. 2

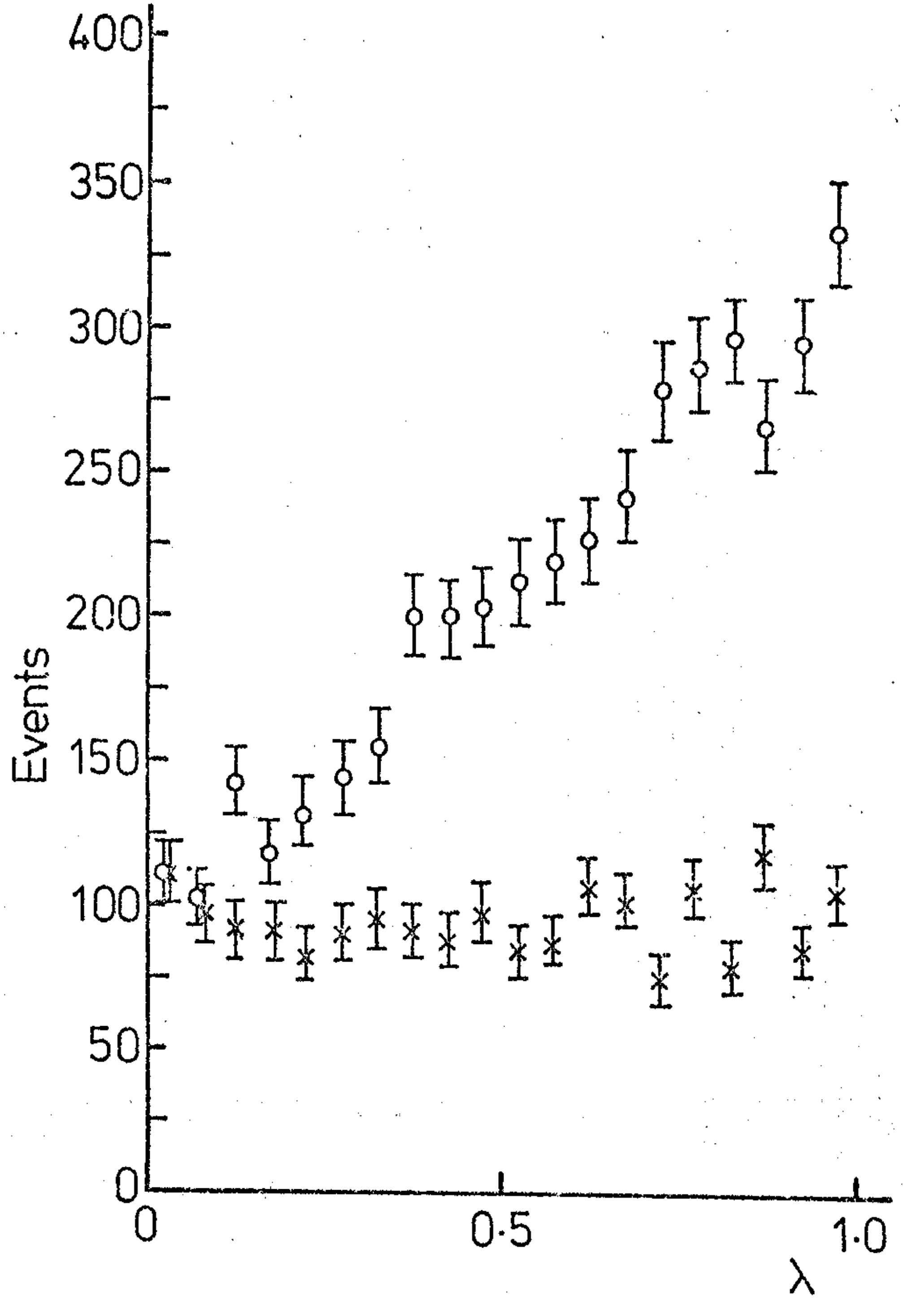

Fig. 3

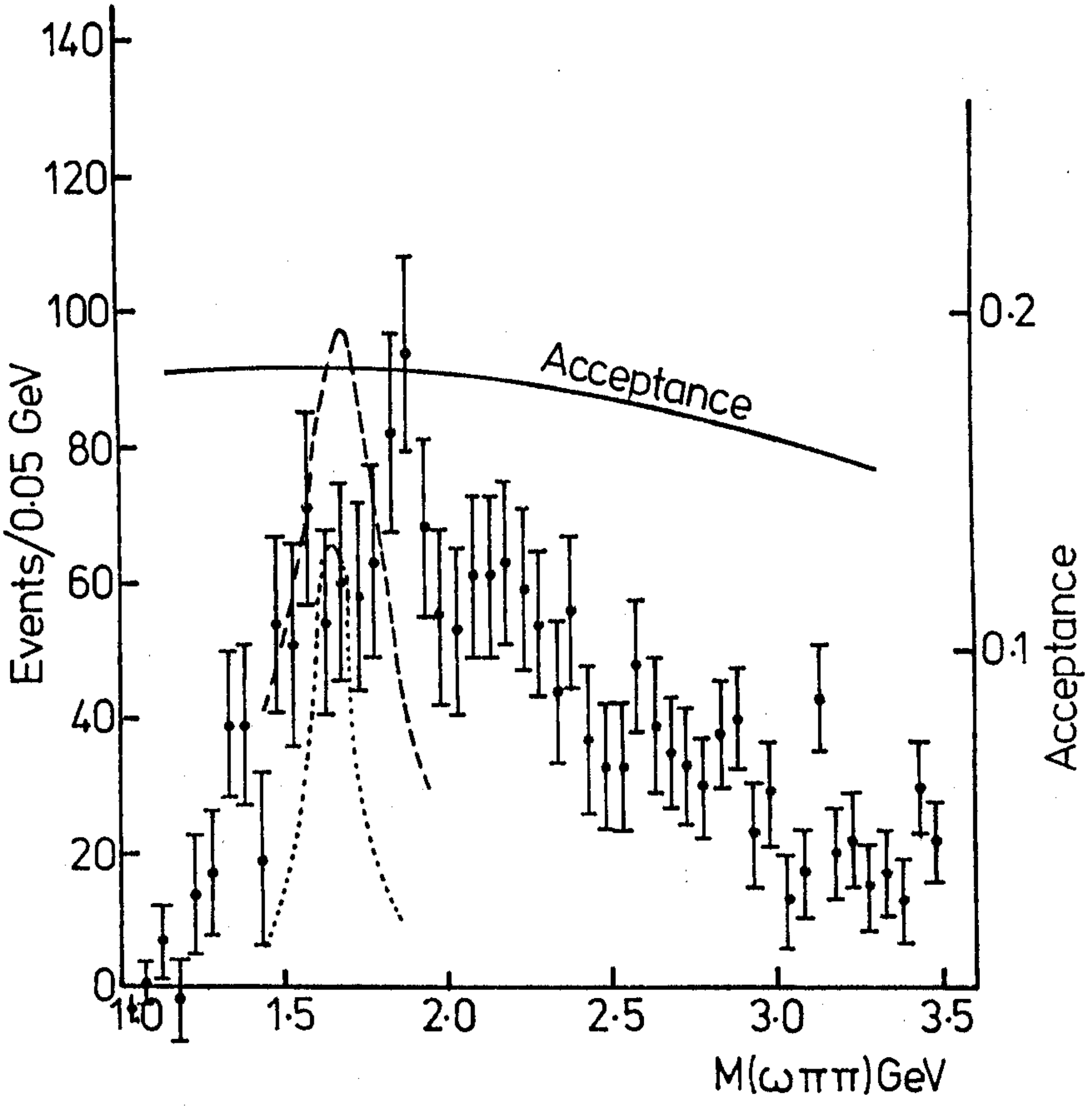
140
120
100
80
60
40
20
0
Events/0.05 GeV
1.0
1.5
2.0
2.5
3.0
3.5
M(ωππ)GeV
Acceptance
0.2
0.1
Acceptance

Fig. 4

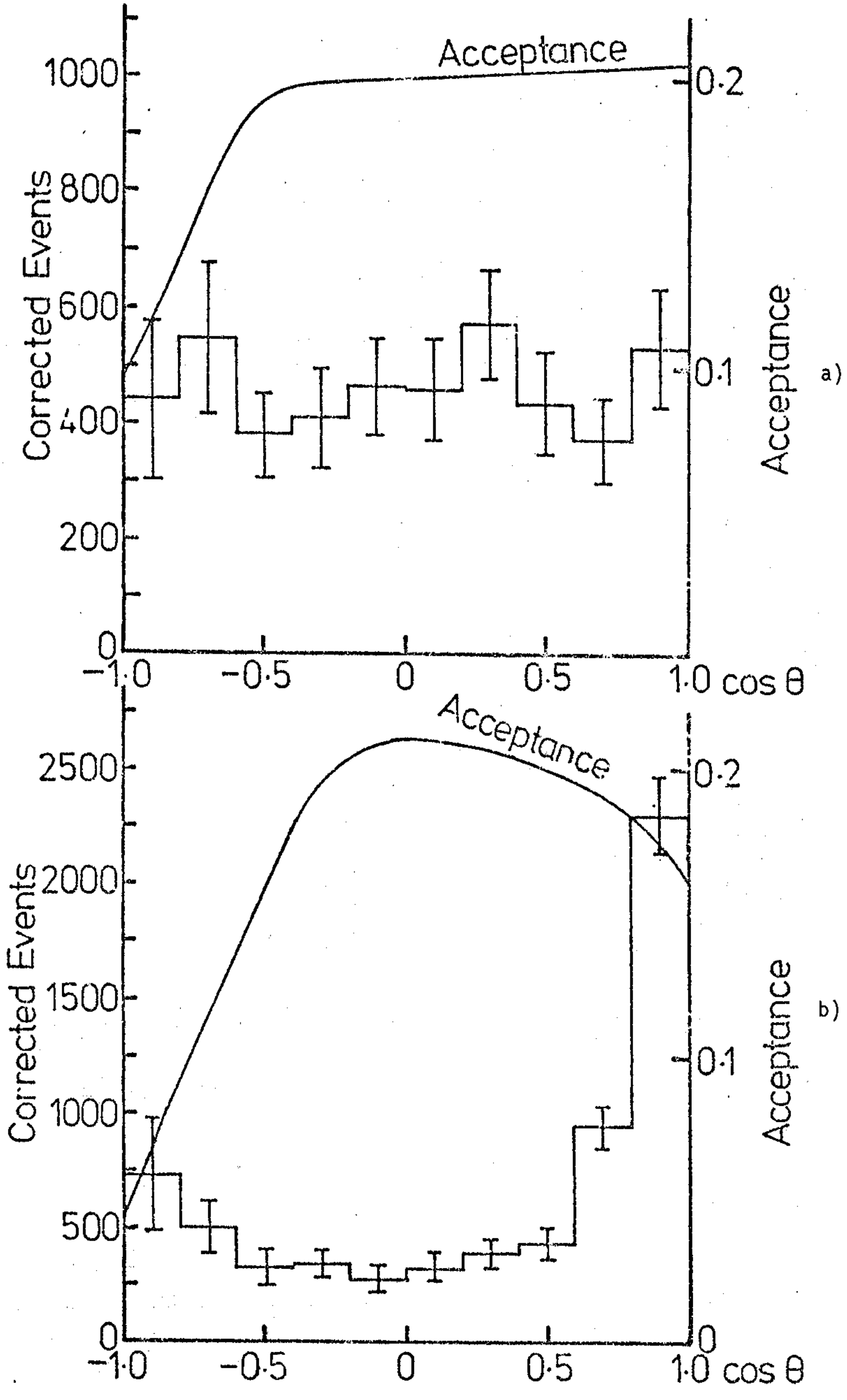
Acceptance
Corrected Events
1000
800
600
400
200
0
0·2
0·1
Acceptance
a)
−1·0
−0·5
0
0·5
1·0 cos θ
Acceptance
Corrected Events
2500
2000
1500
1000
500
0
0·2
0·1
0
Acceptance
b)
−1·0
−0·5
0
0·5
1·0 cos θ

Fig. 5

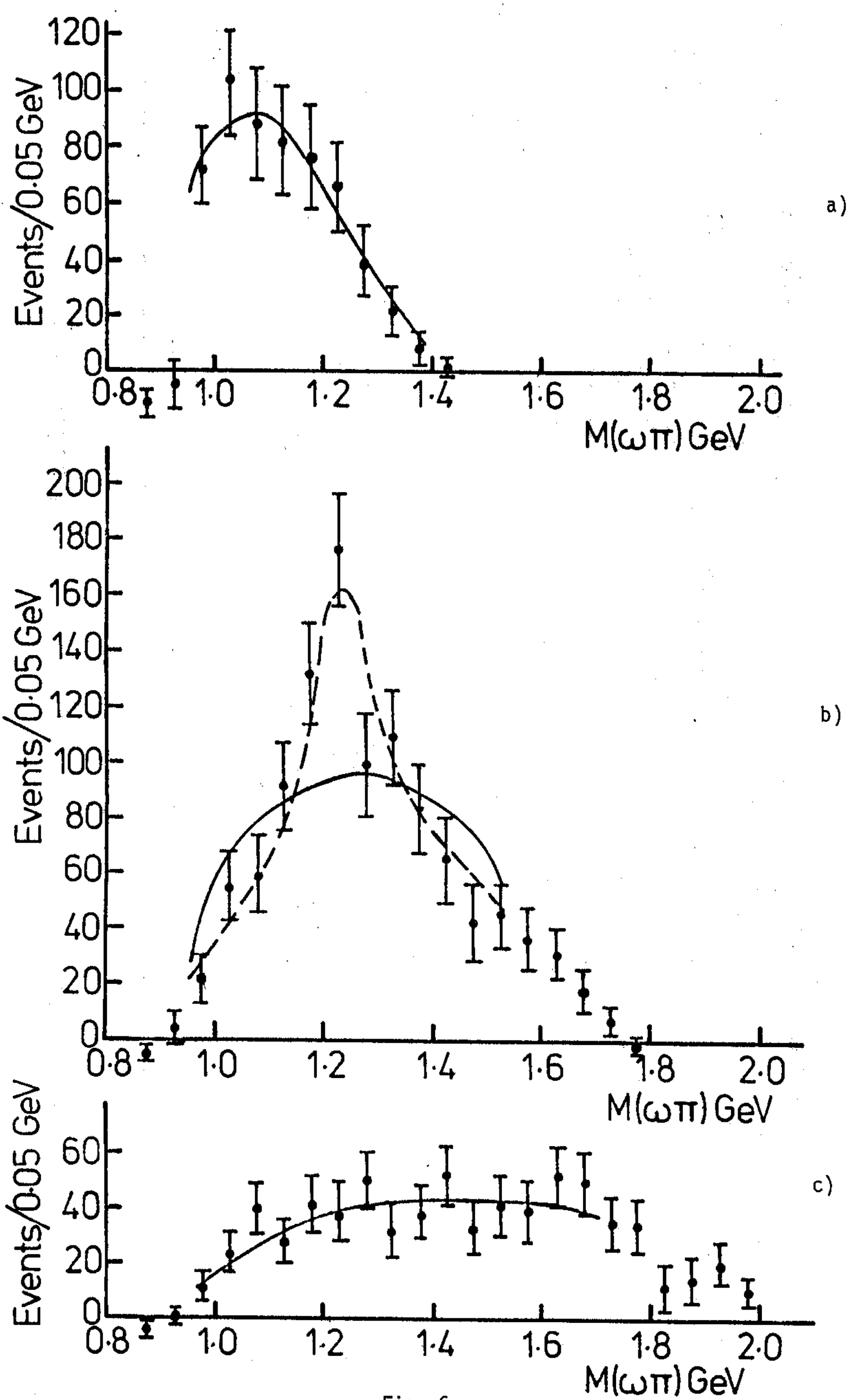
Events/0.05 GeV
120
100
80
60
40
20
0
0.8
1.0
1.2
1.4
1.6
1.8
2.0
M(ωπ) GeV
a)
Events/0.05 GeV
200
180
160
140
120
100
80
60
40
20
0
0.8
1.0
1.2
1.4
1.6
1.8
2.0
M(ωπ) GeV
b)
Events/0.05 GeV
60
40
20
0
0.8
1.0
1.2
1.4
1.6
1.8
2.0
M(ωπ) GeV
c)

Fig. 6

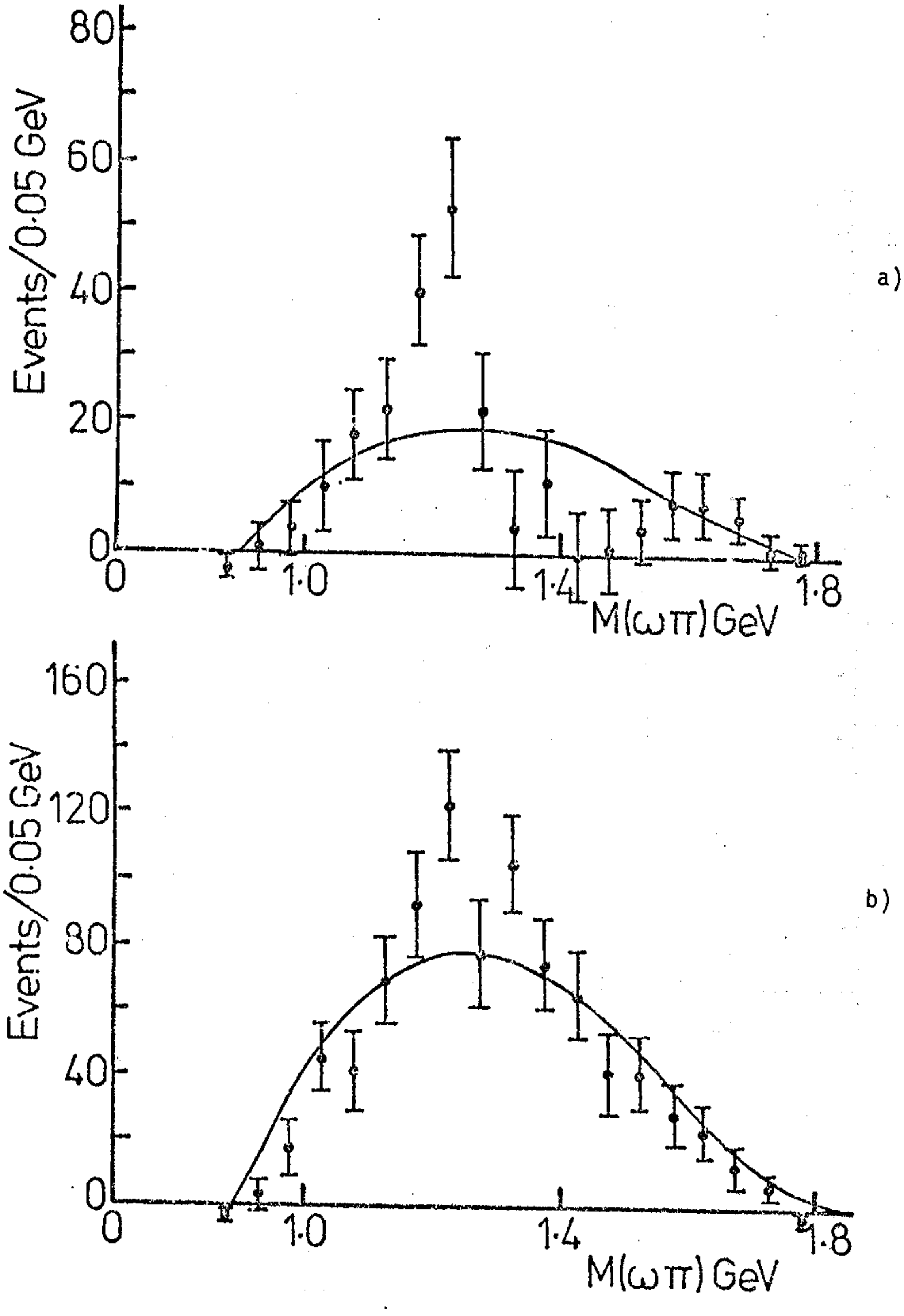
80
60
40
20
0
Events/0·05 GeV
0
1·0
1·4
1·8
M(ωπ) GeV
a)
160
120
80
40
0
Events/0·05 GeV
0
1·0
1·4
1·8
M(ωπ) GeV
b)

Fig. 7

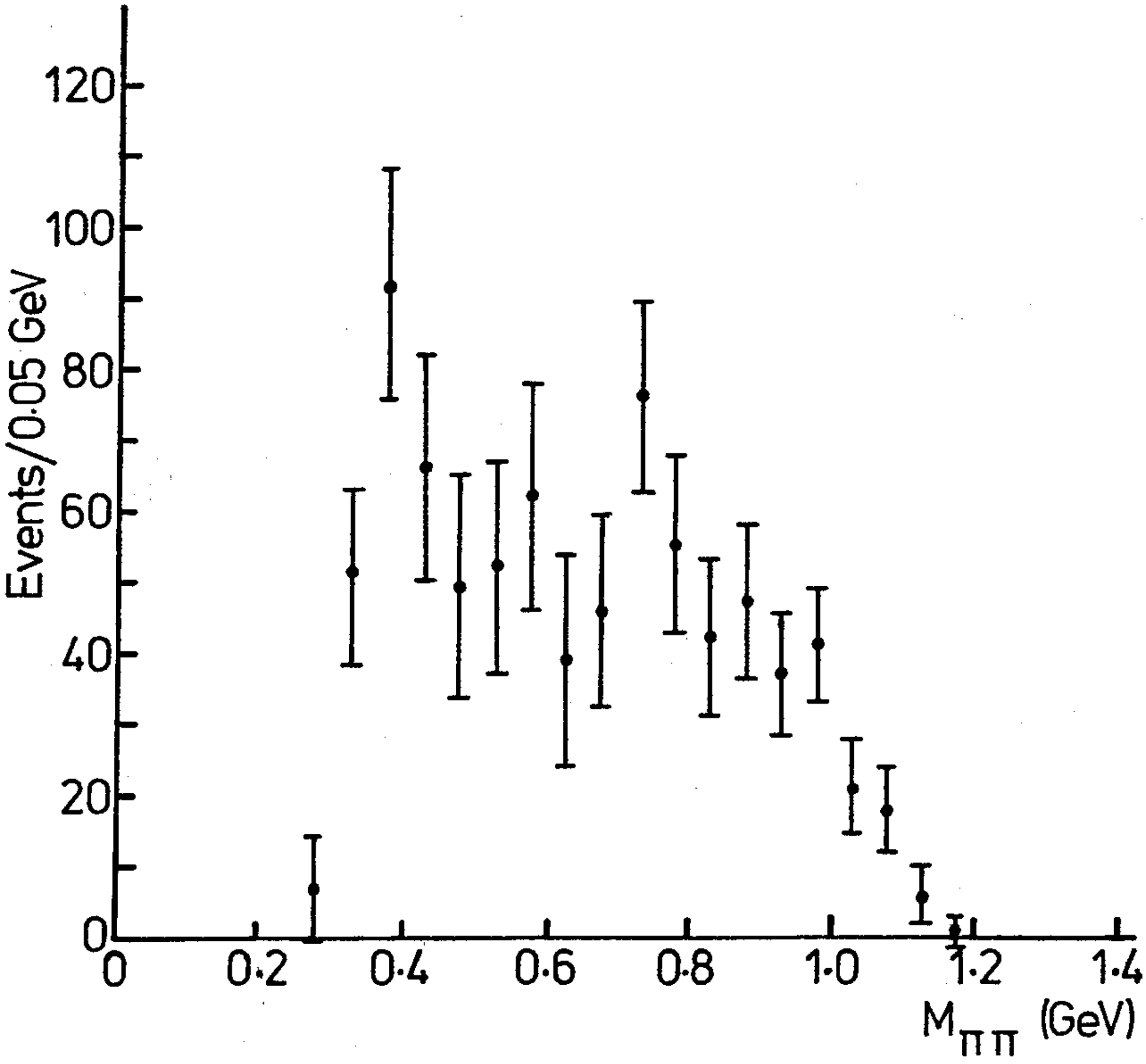

Events/0.05 GeV
120
100
80
60
40
20
0
0
0·2
0·4
0·6
0·8
1·0
1·2
1·4
$M_{\pi\pi}$ (GeV)

Fig. 8

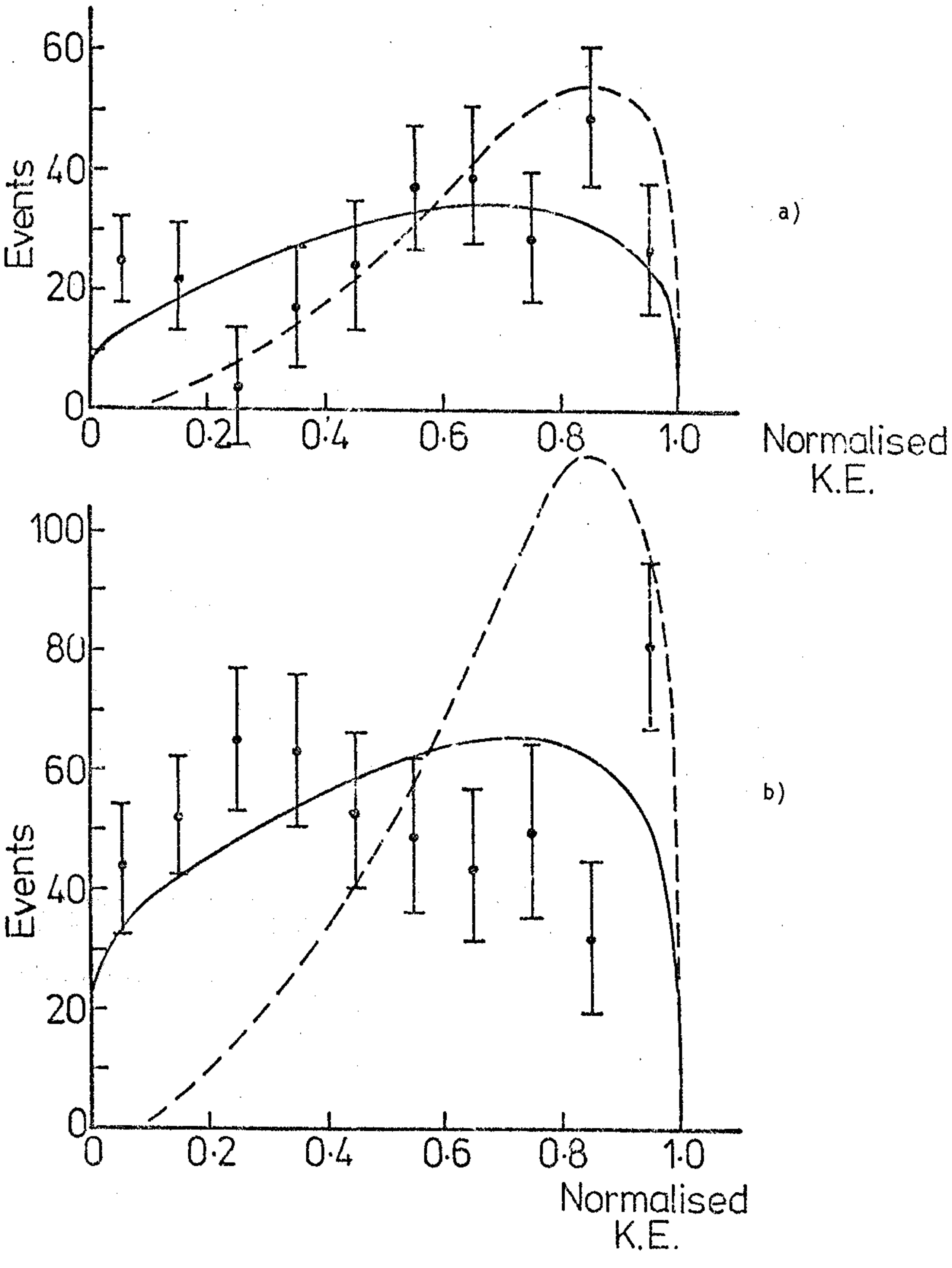
60
40
20
0
Events
0
0·2
0·4
0·6
0·8
1·0
Normalised K.E.
a)
100
80
60
40
20
0
Events
0
0·2
0·4
0·6
0·8
1·0
Normalised K.E.
b)

Fig. 9

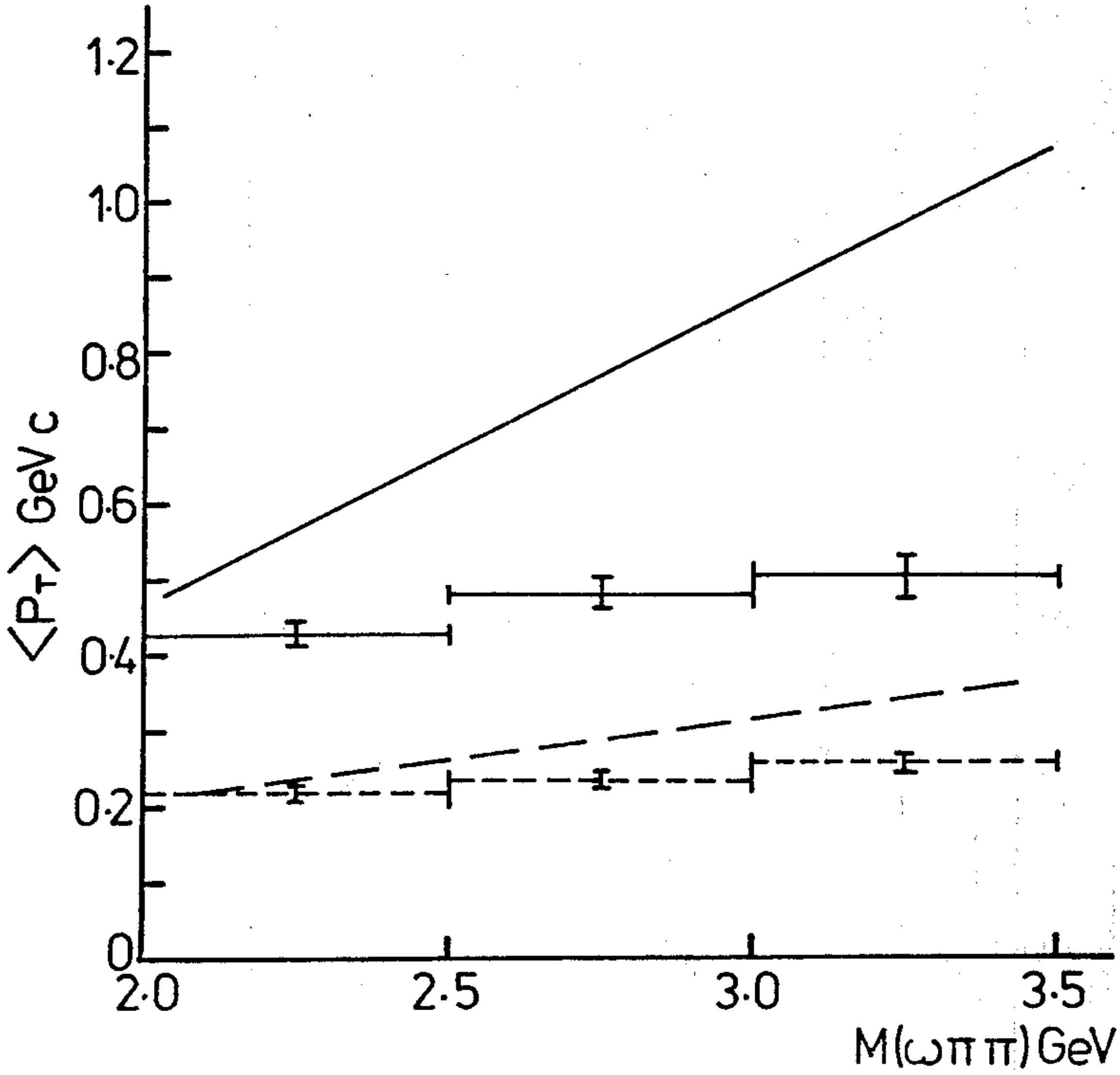

Fig. 10